



# SUPRAMOLECULAR COMPLEXES OF CUCURBITURILS WITH SECOND GROUP METAL SALTS AND HYDRATES AND HISTAMINE

Yu. A. Borisov and S. S. Kiselev\*

*Nesmeyanov Institute of Organoelement Compounds, Russian Academy of Sciences,  
ul. Vavilova 28, Moscow, 119991 Russia*

Cite this: *INEOS OPEN*,  
2021, 4 (2), 70–77  
DOI: 10.32931/io2109a

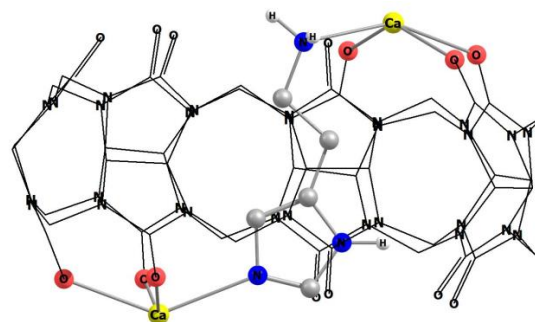
Received 16 February 2021,  
Accepted 4 June 2021

<http://ineosopen.org>

## Abstract

The interaction of cucurbiturils (Q6, Q7, and Q8) with Ca and Ba chlorides and iodides are studied for the first time by density functional theory. The thermodynamic parameters for the formation of host–guest complexes are calculated. The structures of complexes of Q6 and Q7 with one and two guest molecules are established. The energy parameters for the transfer of  $\text{Be}^{2+}$  and  $\text{Ba}^{2+}$  cations from an aqueous solution into the cavity of Q7 containing  $n$  water molecules are defined. The dependences of the formation energies for complexes  $\text{Q7W}_n\text{Be}^{2+}$  and  $\text{Q7W}_n\text{Ba}^{2+}$  on the number of water molecules are shown to be parabolic, with the energy minima at  $n = 5$  and  $n = 6$ , respectively. It is found that Q7 can form in an aqueous solution supramolecular complexes with protonated histamine (HA) and neutral histamine in the presence of  $\text{Ca}^{2+}$  ions.

**Key words:** cucurbiturils, histamine, beryllium, calcium, barium.



## Introduction

Cucurbiturils (Q $n$ ) can readily bind metal cations in aqueous solutions [1–3] owing to the enhanced polarization of oxygen atoms located in the plane of Q $n$  portals. Metal aqua complexes bind with the carbonyl oxygen atoms of Q6 portals, forming caps that effectively enclose both sides of the cavitand interior. The formation of a barrel-shaped supramolecular compound with two caps enables the incorporation and retention of a guest molecule in the cavity. As the system acidity increases, the oxygen atoms of the Q6 portals undergo protonation, the caps are removed, and the guest is released from the cavity.

Depending on the size, the cucurbituril cavity can include 2 to 22 high-energy water molecules (compared to their energies in an aqueous solution) [2]. The water contents in Q5 and Q8 cucurbiturils roughly correspond to its contents in  $\alpha$ - and  $\gamma$ -cyclodextrins, respectively, but in the case of  $\beta$ -cyclodextrin, which can include 6–7 water molecules, there are no matches: Q6 can include 4 and Q7—8 water molecules. Buschmann *et al.* [3] noticed that the solubility of Q6 in neat water is relatively low but increases in the presence of alkali or alkaline earth metal salts.

Recently, we have studied the structuring of water and hydroxonium ions in the Q7 portal by quantum chemistry methods [4]. It was shown that the enthalpy and Gibbs free energy during sequential attachment of water molecules to neutral Q7 passes through two minima at the water molecule content  $n = 4$  and 8. For the protonated cucurbituril, the enthalpy has minima at  $n = 7$  and 10. It was also revealed that complex  $\text{Q7-OH}^+$  with the protonated carbonyl oxygen atom has lower

energy than complex  $\text{Q7-NH}^+$  (by 18 kcal), where the proton is bound with the nitrogen atom. The evaluation of the number of water molecules on carbonyl portals is a nontrivial task due to the possibility of the formation of a complex molecular network as a result of dipole–dipole interactions.

A supramolecular compound of Q6 with sodium aqua complex [5] is the first example of a molecular container that is capable of reversible inclusion of guests, forming and breaking bonds between the metal aqua complex and the macrocycle. Freeman [6] explored a compound of Q6 with calcium aqua complex  $\text{Q6-2[Ca(HSO}_4)_2] \cdot 13\text{H}_2\text{O}$ . It represents a polymer that consists of the alternating molecules of Q6 bound with calcium cations through the carbonyl groups. In the presence of methanol, the latter is readily included in the cavity without changing the supramolecular packing.

Some technological accidents result in the discharge of long-living radioactive isotopes of Cs, Sr, and I into the environment, which are highly dangerous for humans and all living organisms. Pichierri [7] performed DFT calculations and crystallographic analysis of the binding of hydrated  $\text{Cs}^+$  ions with Q $n$ , where  $n = 5$ –8, and discussed the potential of application of cucurbiturils for ecological deactivation of cesium radionuclides.

The first DFT calculations of the complexes of Q6 with alkaline earth metal cations were performed by Sinha and Sundararajan [8] who showed that the metal cation is located in an anionic part of the Q6 portal in a supramolecular complex at the same distances from the carbonyl oxygen atoms.

Zhang *et al.* [9] emphasized the role of investigations on supramolecular cucurbituril complexes in improving the quality

and energy efficiency of some important industrial separation processes. It was reported that the separation of *ortho*-disubstituted benzenes using an aqueous solution of Q7 proceeds with selectivity above 92%. The theoretical host–guest models showed that the *ortho*-isomer with the lowest ratio of sides fits in well with the spherical interior of Q7, which leads to very stable complexes. Furthermore, laboratory experiments on scaling with commercial xylenes and an aromatic fraction of pyrolysis gasoline confirmed that Q7 can extract *ortho*-xylene with the perfect selectivity of up to 83%.

Lambert *et al.* [10] marked the promising role of Q6 as a catalyst for isomerization of [*m*-xylene + H]<sup>+</sup> into [*p*-xylene + H]<sup>+</sup> under vacuum. It is expected that the macrocycle can accelerate the rate of isomerization at 500 K by two orders of magnitude owing to the stabilization of a transient state upon simultaneous inhibition of a competing reaction. In contrast, Q7 is not expected to be a high-performance catalyst for these reactions.

The complexes of Qn with biologically active molecules [11, 12] are one of the most popular research objects in the chemistry of inclusion compounds. This is connected with entirely new properties of these complexes compared to those of the guest molecules. Thus, the enhanced solubility of organic molecules in the composition of these complexes in aqueous solutions was detected. The stability of organic molecules in physiological solutions is improved during storage. The pharmacological activity and duration of the therapeutic effect of drugs also increase. The new chromophoric properties are manifested.

The interaction of biologically important metal cations (Na<sup>+</sup>/K<sup>+</sup> and Mg<sup>2+</sup>/Ca<sup>2+</sup>) with Qn (n = 6–8) was studied by DFT calculations using the M062X functional, which allowed for evaluating the main factors that define complex formation [13]. Molecular modeling (MD) and several spectroscopic techniques were used to analyze the intermolecular interactions in binary and ternary systems based on Q7, DNA, and a bis(styryl) dye [14]. Fedorova *et al.* [15] described a four-component system bearing bis(styryl) dyes, HP-β-CD (modified cyclodextrin), and Q7. The complexes of the bis(styryl) dyes and Q7 in these systems responded to the changes in pH and concentration of Ba<sup>2+</sup> ions, which led to dissociation of the bis(styryl) complexes, resulting in the formation of Q7·Ba<sup>2+</sup> complexes.

The interaction between inverted Q7 (iQ7) and six biogenic amines, namely, tyramine, 2-phenylethylamine, HA, tryptamine, spermine, and spermidine were studied by the <sup>1</sup>H NMR, UV-vis and fluorescence spectroscopy, calorimetry, and mass spectrometry [16]. The results obtained suggest that iQ7 forms supramolecular complexes with five of these biogenic amines, except for HA, and the binding sites of the host–guest complexes depend on the structure of the biogenic amine.

Histamine plays an important physiological role in the body but, at the same time, it is the most toxic one among all biogenic amines. The use of products containing significant concentrations of HA can cause unfavorable organism reactions (neurological, respiratory, and gastrointestinal). The high content of histamine was detected, for example, in blue cheese [17].

The goal of this work is to investigate the interaction of Ca and Ba chlorides and iodides with cucurbiturils Q6, Q7, and Q8 in the gas phase as well as the interaction of Q7 with aqua

complexes of metal cations (Be<sup>2+</sup>, Ba<sup>2+</sup>) in aqueous solutions. The structures and energy of formation of supramolecular complexes of Q7 with mono- and diprotonated HA, as well as neutral HA in the presence of Ca<sup>2+</sup> ions in water were studied for the first time.

## Results and discussion

Table S1 in the Electronic Supplementary Information (ESI) presents the results of the calculation of the energies of the compounds and inclusion complexes under consideration. Here E<sub>tot</sub> is the total energy of a molecular system.

$$E_{\text{zpve}} = E_{\text{tot}} + \text{ZPVE}$$

$$E_{\text{H}} = E_{\text{tot}} + \text{ZPVE} + E_{\text{vib}} + E_{\text{rot}} + E_{\text{trans}}$$

$$E_{\text{G}} = E_{\text{H}} - T \cdot S$$

ZPVE is the zero-point vibration energy, E<sub>vib</sub> is the vibration energy, E<sub>rot</sub> is the rotation energy, E<sub>trans</sub> is the translation energy, S is the entropy, and T is the temperature on the Kelvin scale.

### Structure of a complex of Q6 with one and two molecules of CaCl<sub>2</sub>

Figure 1 depicts the structure of a complex of Q6 with one molecule of CaCl<sub>2</sub>.

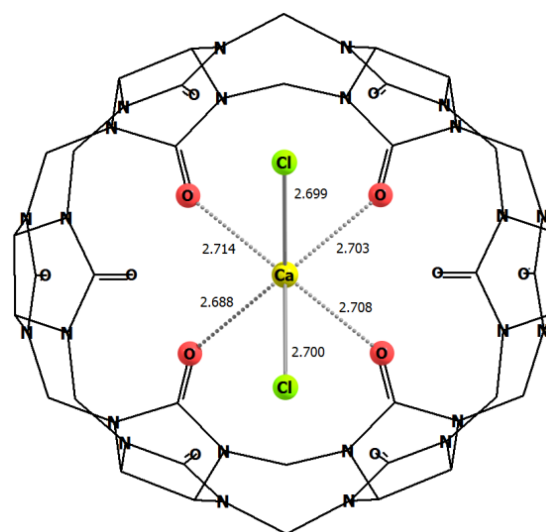
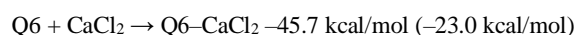


Fig. 1. Structure of the complex of Q6 with one molecule of CaCl<sub>2</sub>. Hereinafter, the interatomic distances are given in angstroms.

In this complex, the calcium atom is coordinated with four oxygen atoms of the cucurbituril carbonyl groups. The Ca–O distances are equal to 2.7 Å. The remaining two carbonyl oxygen atoms are separated from the Ca center at much longer distances (4.7 Å). The angle Cl–Ca–Cl is equal to 109.0 deg. The following energies were obtained for this complex: E(HOMO) = –0.1933 a. u. and E(LUMO) = 0.0001 a. u. The APT effective charge is equal to +1.68 e, the charge on the chlorine atoms is –0.83 e, and that on the four oxygen atoms coordinated with the calcium atom is –0.80 e. Using the data from Table S1, the thermodynamic characteristics of the formation of the complex Q6–CaCl<sub>2</sub> can be calculated according to the following reaction:



The first value corresponds to the reaction enthalpy, while the second one in parentheses—to the Gibbs free energy change.

Figure 2 presents the structure of a complex of Q6 with two molecules of  $\text{CaCl}_2$ . Each molecule of  $\text{CaCl}_2$  forms coordination bonds with four or two oxygen atoms of the cucurbituril carbonyl groups.

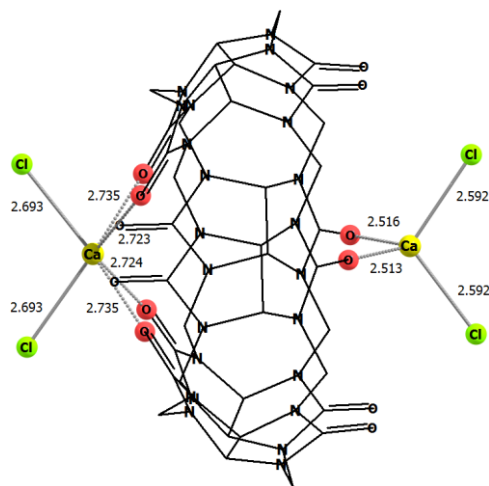
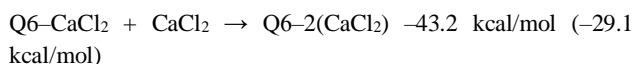


Fig. 2. Structure of the complex of Q6 with two molecules of  $\text{CaCl}_2$  (I).

This complex features the following parameters:  $E(\text{HOMO}) = -0.2076$  a. u. and  $E(\text{LUMO}) = -0.0228$  a. u. Both  $\text{CaCl}_2$  molecules enclose the entries to the Q6 cavity. The effective charges on the metal atoms are equal on average to  $+1.63$  e, that on the chlorine atoms is  $-0.81$  e, and the charge on the oxygen atoms coordinated with the calcium atom is  $-0.83$  e. Using the data from Table S1, the thermodynamic characteristics of the formation of the complex  $\text{Q6-2}(\text{CaCl}_2)$  can be calculated according to the following reaction:



The first value refers to the reaction enthalpy, the second one in parentheses—to the Gibbs free energy change.

Complex **I** depicted in Fig. 2 is more feasible in the presence of guests in the Q6 cavity. However, if there are no guests, complex **II** appears to be more stable (by 18 kcal/mol). The structure of **II** is shown in Fig. 3. The calculated energies for this complex are as follows:  $E(\text{HOMO}) = -0.1786$  a. u. and  $E(\text{LUMO}) = -0.0101$  a. u. One  $\text{CaCl}_2$  molecule encloses the interior of Q6, while the chloride anion of the second one enters the Q6 cavity, forming a coordination bond with the calcium atom of the former  $\text{CaCl}_2$  molecule. For the former molecule of  $\text{CaCl}_2$ , the effective charge on the calcium atom is  $+1.63$  e and that on the chlorine atoms is  $-0.83$  e. For the second molecule of  $\text{CaCl}_2$ , the effective charge on the calcium atom is  $+1.59$  e, the charge on the chlorine atom in the center of Q6 is  $-0.67$  e, and that on the second chlorine atom is  $-0.82$  e.

Using the data from Table S1, the thermodynamic characteristics of the formation of the complex  $\text{Q6-2}(\text{CaCl}_2)$  can be calculated according to the following reaction:

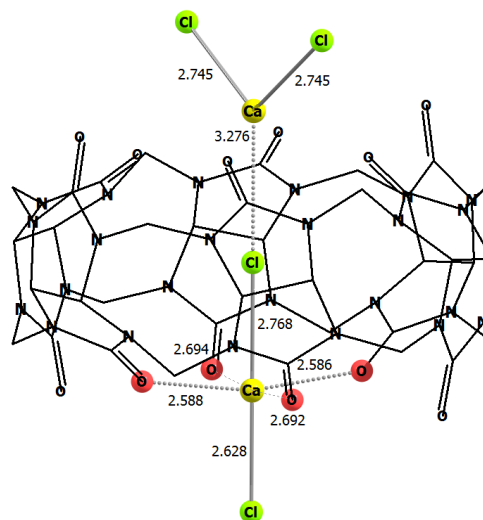
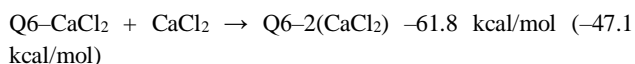


Fig. 3. Structure of the complex of Q6 with two molecules of  $\text{CaCl}_2$  (II).

### Structure of the complex of Q6 with two molecules of $\text{BaI}_2$

Figure 4 shows the structure of a complex of Q6 with two molecules of  $\text{BaI}_2$ . The following energy parameters were calculated for this complex:  $E(\text{HOMO}) = -0.1485$  a. u. and  $E(\text{LUMO}) = -0.0358$  a. u. One molecule of  $\text{BaI}_2$  encloses the entry to the Q6 interior, whereas the iodide anion of the second one enters its cavity, forming a coordination bond with the barium atom of the former  $\text{BaI}_2$  molecule. For the former molecule of  $\text{BaI}_2$ , the effective charge on the barium atom is  $+1.61$  e and that on I is  $-0.84$  e. For the second molecule of  $\text{BaI}_2$ , the effective charge on the barium atom is  $+1.60$  e, the charge on the iodine atom in the center of Q6 is  $-0.61$  e, and that on the second iodine atom is  $-0.79$  e. Using the data from Table S1, the thermodynamic characteristics of the formation of the complex  $\text{Q6-2}(\text{BaI}_2)$  can be calculated according to the following reaction:

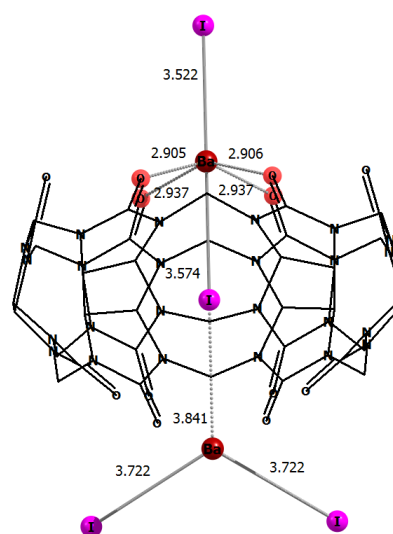
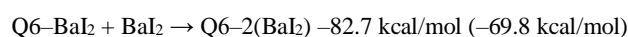


Fig. 4. Structure of the complex of Q6 with two molecules of  $\text{BaI}_2$ .

### Structure of complexes of Q7 and Q8 with one molecule of $\text{BaI}_2$

Figure 5 depicts the structure of a complex of Q7 with one molecule of BaI<sub>2</sub>. In this case, the molecule of BaI<sub>2</sub> is arranged unsymmetrically relative to the entry to the Q7 cavity and forms only four bonds with the O=C groups of the cavitand, with the bond lengths ranging within 2.83–2.86 Å. The angle I–Ba–I is equal to 125.0 deg. The formation of the bonds between Q7 and BaI<sub>2</sub> leads to the distortion of a cylindrical shape of the cucurbituril, which can be seen from Fig. 5.

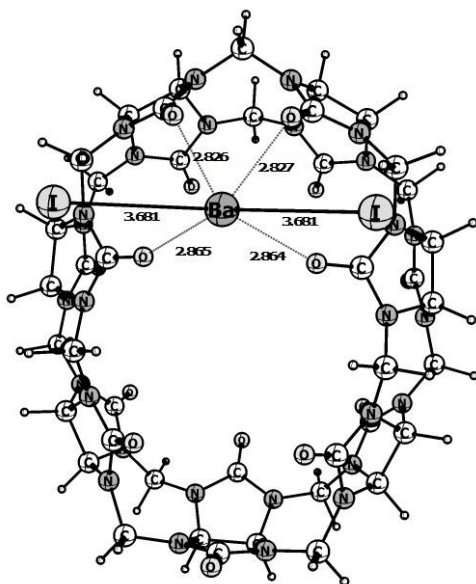


Fig. 5. Structure of the complex of Q7 with one molecule of BaI<sub>2</sub>.

Figure 6 demonstrates the structure of a complex of Q8 with one molecule of BaI<sub>2</sub> and presents the lengths of the bonds between the Ba atom and the carbonyl oxygen or iodine atoms. The distortion of the Q8 structure in this complex is also apparent.

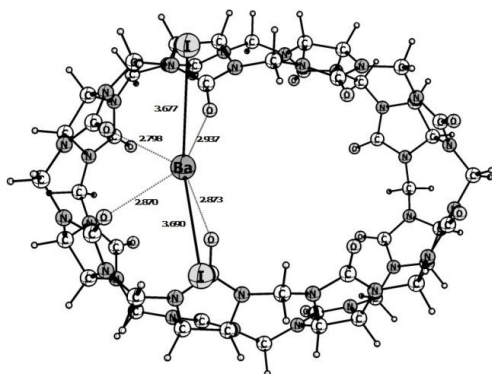


Fig. 6. Structure of the complex of Q8 with one molecule of BaI<sub>2</sub>.

### Thermodynamic parameters of the complex formation between Q6, Q7, Q8 and BaI<sub>2</sub>

Table 1 lists the thermodynamic characteristics (enthalpy  $\Delta H$ , Gibbs free energy  $\Delta G$ , and entropy  $\Delta S$ ) for the following reaction, which were calculated based on the data from Table S1:  $Q_n + BaI_2 \rightarrow Q_n-BaI_2$  (1)

Table 1. Thermodynamic characteristics of reaction (1)

n	$\Delta H$ , kcal/mol	$\Delta G$ , kcal/mol	$\Delta S$ , kcal/(mol·K)
6	-77.9	-63.1	-49.8
7	-67.2	-52.6	-49.3
8	-61.9	-46.2	-47.4

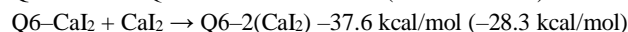
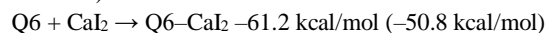
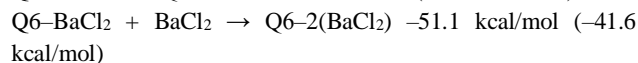
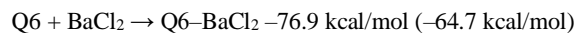
As can be seen from Table 1, while passing from  $n = 8$  to  $n = 6$ , the energy gain during complex formation increases by 16 kcal. For the complex with  $n = 8$ , the angle I–Ba–I composes 124.2 deg and the dipole moment is equal to 10.2 D. For the complex with  $n = 6$ , the angle I–Ba–I composes 117.2 deg and the dipole moment is equal to 15.1 D. These data suggest that, in the complex with  $n = 6$ , the electrostatic forces pull the metal ion inside the cucurbituril interior and push the iodine ions out of this area. The additional calculations showed that the dipole moments of the complexes  $Q_n-BaI_2$  are created exclusively owing to the salt, whereas the cucurbituril itself almost does not contribute to the dipole moment of the complex.

### Thermodynamic parameters of the complex formation between Q6 and BaCl<sub>2</sub> or CaI<sub>2</sub>

In the complex of BaCl<sub>2</sub> with Q6, the barium atom is coordinated with four oxygen atoms of the cucurbituril carbonyl groups. The Ba–O distances are equal to 2.85 Å. The remaining two oxygen atoms of the carbonyl moieties are separated from the barium atom at much longer distances (4.63 Å). Both of the Ba–Cl distances are equal to 3.16 Å. The angle Cl–Ba–Cl is 126.9 deg. The following energy parameters were calculated for this complex:  $E(\text{HOMO}) = -0.1750$  a. u. and  $E(\text{LUMO}) = -0.01146$  a. u. The APT effective charge on the barium atom is +1.69 e, the charge on the chlorine atoms is -0.85 e, and that on the oxygen atoms coordinated with the barium atom is -0.79 e.

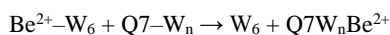
In the complex of CaI<sub>2</sub> with Q6, the calcium atom is coordinated with four oxygen atoms of the cucurbituril carbonyl groups. The Ca–O distances are equal to 2.6 Å. The remaining oxygen atoms of the O=C groups are separated from the Ca atom at much longer distances (4.6 Å). Both Ca–I distances are equal to 3.31 Å. The angle I–Ca–I is 102.1 deg. This complex features the following energies:  $E(\text{HOMO}) = -0.1607$  a. u. and  $E(\text{LUMO}) = -0.0255$  a. u. The APT effective charge on the calcium atom is equal to +1.62 e, the charge on the iodine atoms is -0.80 e, and that on the oxygen atoms coordinated with the calcium atom is -0.82 e.

The thermodynamic characteristics calculated based on the data from Table S1 are presented below (enthalpy  $\Delta H$ , Gibbs free energy  $\Delta G$ , and entropy  $\Delta S$ ):



### Thermodynamic parameters of the transfer of Be<sup>2+</sup> ions from an aqueous solution into the Q7 cavity

In an aqueous solution, Q7 can retain in its cavity up to 8 structured water molecules [4]. We calculated the thermodynamic parameters of the transfer of Be<sup>2+</sup> cations from an aqueous solution into the hydrated Q7 cucurbituril according to the following model reaction:



The beryllium cation in an aqueous medium was modeled in the form of an aqueous cluster bearing six water molecules. Figure 7 depicts the dependence of the enthalpy  $\Delta H$  and Gibbs free energy  $\Delta G$  for this reaction on the number of water molecules in the Q7 cavity.

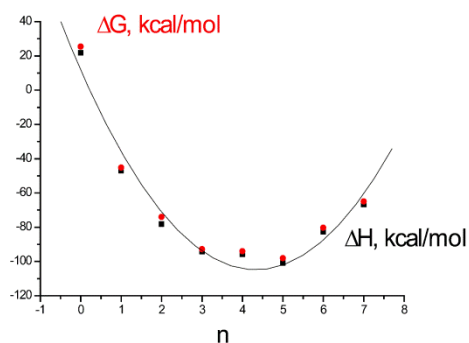


**Fig. 7.** Dependence of  $\Delta H$  (black marks) and  $\Delta G$  (red marks) in kcal/mol on the number of water molecules ( $n$ ) in the Q7 cavity.

The dependences of the enthalpy and Gibbs free energy have the parabolic forms with the minima at  $n = 5$ . Figure 8 depicts the structure of complex  $\text{Q7W}_5\text{Be}^{2+}$ .

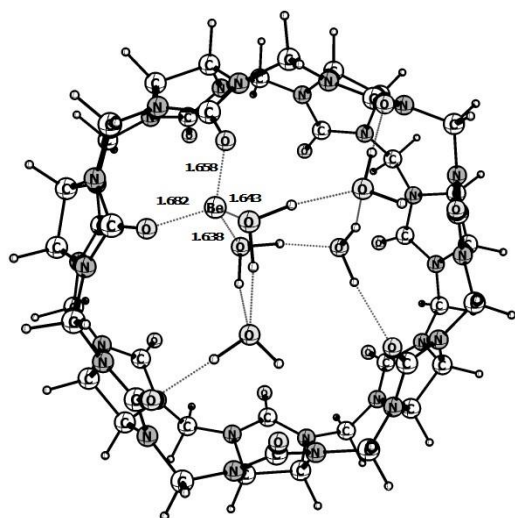


**Fig. 8.** Structure of the complex  $\text{Q7W}_5\text{Be}^{2+}$ .

### Energy parameters of the transfer of $\text{Ba}^{2+}$ ions from an aqueous solution into the Q7 cavity

We also considered the energy of transfer of  $\text{Ba}^{2+}$  cations from an aqueous solution into the hydrated Q7 interior according to the following reaction:

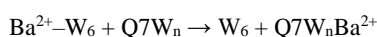
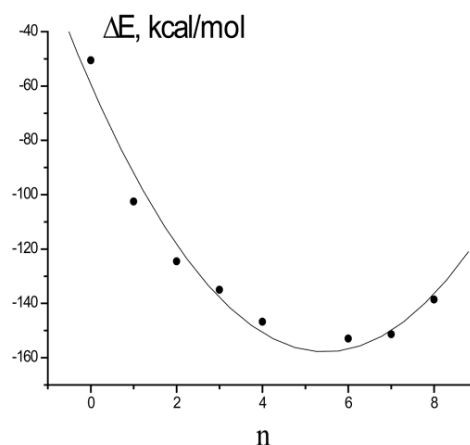
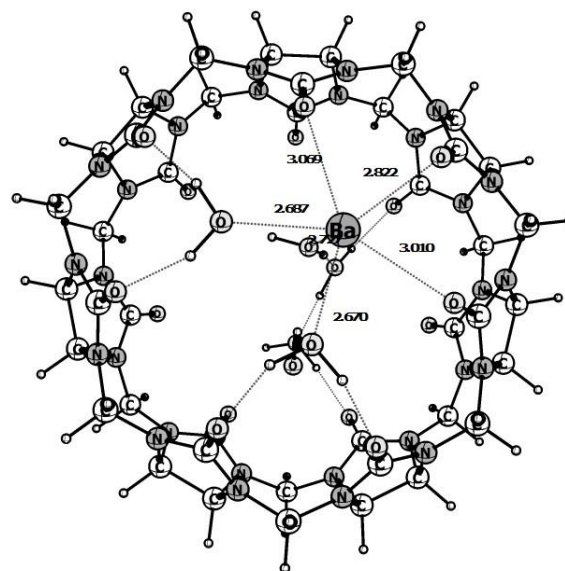


Figure 9 presents the dependence of the total formation energy of  $\text{Q7W}_n$  with doubly charged  $\text{Ba}^{2+}$  ions on the number of water molecules ( $n$ ) in the Q7 cavity. Dependence has an almost squared shape. The energy minimum is located at  $n = 6$ .



**Fig. 9.** Dependence of the energy of interaction (in kcal/mol) between  $\text{Q7W}_n$  and doubly charged  $\text{Ba}^{2+}$  ions on the number of water molecules ( $n$ ) in Q7.

Figure 10 depicts the structure of the complex  $\text{Q7W}_6\text{Ba}^{2+}$  and some distances (in angstroms).



**Fig. 10.** Structure of complex  $\text{Q7W}_6\text{Ba}^{2+}$ .

### Energy parameters of the complex formation between Q7 and HA and $\text{Ca}^{2+}$ in an aqueous solution

Table S2 (ESI) lists the main results of calculations for the complexes of Q7 with HA and  $\text{Ca}^{2+}$  in water. Q7 can retain up to 8 high-energy structured water molecules in its cavity [4] (reaction 1, Table 2). Using the data from Table S2, we calculated the thermodynamic characteristics of the transfer of neutral HA from an aqueous solution into the hydrated Q7 cavity by model reaction 2 (Table 2) using the B3LYP-D3 and wB97xD (in parentheses) functionals:  $\Delta H = +15.1$  (9.5) kcal/mol,  $\Delta G = +9.1$  (4.1) kcal/mol.

The values of enthalpy  $\Delta H$  and Gibbs free energy  $\Delta G$  are positive and, consequently, the process of cluster substitution consisting of 8 water molecules ( $\text{W}_8$ ) for neutral HA inside the Q7 cavity is energetically unfavorable.

We also calculated the energy of complex formation between Q7 and HA in the presence of hydrated  $\text{Ca}^{2+}$  cations according to reaction 3 (Table 2):  $\Delta H = -9.3$  kcal/mol,  $\Delta G = -7.0$  kcal/mol. The results obtained suggest that the reaction undergoes an equilibrium shift to the formation of a complex of Q7 with neutral HA and two  $\text{Ca}^{2+}$  cations (Fig. 11). In this complex, the  $\text{Ca}^{2+}$  ions form coordination bonds with the oxygen atoms of the cucurbituril carbonyl groups and nitrogen atoms of HA and block HA inside the hydrophobic cavity of Q7.

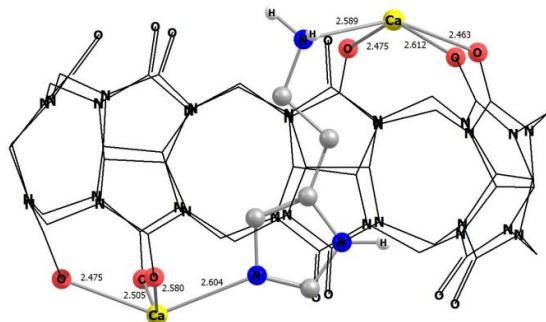


**Fig. 11.** Structure of the complex of Q7 with neutral HA and two  $\text{Ca}^{2+}$  cations.

Biogenic amine HA forms mono- and diprotonated cations in water [18]. Using the data from Table S2, we calculated the thermodynamic parameters of the complex formation between Q7 and mono- and diprotonated HA (Fig. 12) in an aqueous solution according to reaction 4 (Table 2):  $\Delta H = -33.0$  kcal/mol,  $\Delta G = -38.5$  kcal/mol, and the same parameters for reaction 5 (Table 2):  $\Delta H = -33.5$  kcal/mol,  $\Delta G = -30.0$  kcal/mol. The formation of the complex between Q7 and protonated HA in an aqueous solution is energetically favorable owing to the electrostatic interaction and formation of medium hydrogen bonds between the amino group and imidazole ring of HA and the cucurbituril carbonyl groups. According to the hydrogen bond classification [19], the medium A–H–B hydrogen bond has the energies from 4.0 to 14.0 kcal/mol and is characterized by the following parameters: H–B distance within 1.5–2.2 Å, A–B distance within 2.5–3.2 Å, and A–H–B angle within 130–180 deg.

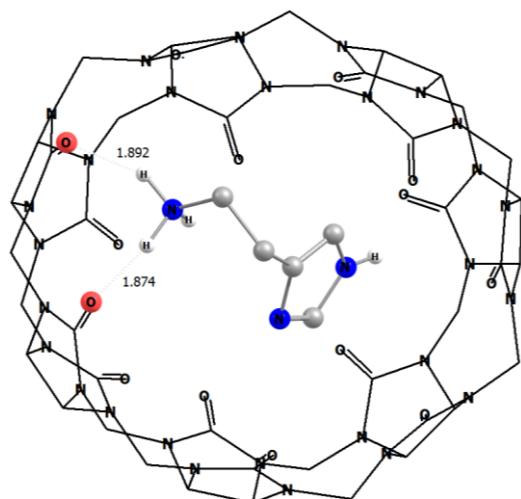


**Fig. 12.** Structure of the complex of Q7 with protonated HA.

Furthermore, according to the thermodynamic parameters, Q7 can form supramolecular complexes with mono- and diprotonated HA and  $\text{Ca}^{2+}$  cations (Fig. 13) by reactions 6 and 7 (Table 2).

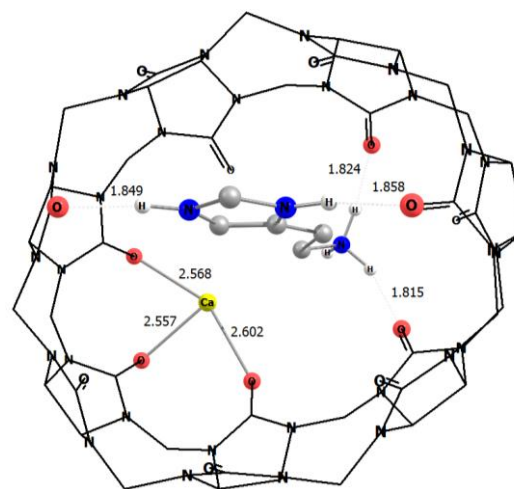


**Fig. 13.** Structure of the complex of Q7 with diprotonated HA and one  $\text{Ca}^{2+}$  cation.

Hence, in aqueous solutions, mono- and diprotonated or neutral HA are arranged in the Q7 container in the bound state, resulting in supramolecular complexes. In other words, this means that Q7 exhibits a histamine-binding effect in aqueous solutions.

**Table 2.** Thermodynamic parameters of the complex formation between Q7 and HA and  $\text{Ca}^{2+}$  ions in water (functionals B3LYP-D3BJ and  $\omega$ B97xD (in parentheses), basis 6-31G(d), solvation model SMD)

Reaction	$\Delta G$ , kcal/mol	$\Delta H$ , kcal/mol	$\Delta S$ , cal/(mol·K)
1 $\text{Q7} + \text{W}_8 \rightarrow \text{Q7-W}_8$	-24.2 (-17.8)	-45.6 (-36.1)	-71.7 (-61.6)
2 $\text{Q7-W}_8 + \text{HA} \rightarrow \text{Q7-HA} + \text{W}_8$	9.1 (4.1)	15.1 (9.5)	20.1 (17.9)
3 $\text{Q7-HA} + 2\text{Ca}^{2+} + \text{W}_8 + 2\text{W}_6 \rightarrow \text{Q7-HA-2Ca}^{2+} + \text{W}_8 + \text{H}_3\text{O}^+$	-7.0	-9.3	-7.5
4 $\text{Q7-HA-H}^+ + \text{W}_8 + \text{H}_2\text{O} \rightarrow \text{Q7-HA-H}^+ + \text{W}_8 + \text{H}_2\text{O}$	-38.5	-33.0	18.6
5 $\text{Q7-HA-H}^+ + \text{H}_3\text{O}^+ \rightarrow \text{Q7-HA-2H}^+ + \text{H}_2\text{O}$	-32.0	-33.5	-5.0
6 $\text{W}_6 \rightarrow \text{Q7-HA-H}^+ + \text{Ca}^{2+} + \text{W}_6$	-6.5	-10.6	-13.7
7 $\text{W}_6 \rightarrow \text{Q7-HA-2H}^+ + \text{Ca}^{2+} + \text{W}_6$	-4.3	-7.7	-11.3

We performed also additional calculations for the complexes of Q7 with histamine, two calcium cations, and 1–5 water molecules given in the explicit form. The results of this investigation are presented in Table S3 in ESI. It was established that the cavity of Q7 can include up to 4 water molecules simultaneously with histamine; the fifth and further water molecules are arranged outside the Q7 cavity. The structure of the complex with 4 water molecules is depicted in Fig. S1 in ESI.

## Computations

The calculations were performed by DFT [20] and DFT-D3 (the empirical dispersion correction D3BJ was used) methods at the B3LYP [21, 22] and  $\omega$ B97XD [23] levels using the 6-31G(d) and LanL2DZ bases. All the computations with the full optimization of molecule geometries and calculation of normal coordinates were carried out using GAUSSIAN09 software [24] running under LINUX operating system. Earlier this approach was successfully used to study the supramolecular complexes of cyclodextrins with organic molecules [25–27] and optical isomers of ferrocene derivatives [28, 29]. The effective charges on atoms in the resulting complexes were calculated using the APT (atomic polarizability tensor) method [30]. To construct the initial model of Q7 with HA, we used a conformer of HA [31] with the minimum energy and preliminarily optimized geometry (B3LYP/6-311++G(d,p)). The geometries of the complexes of Q7 with HA and  $\text{Ca}^{2+}$  in water were optimized twice using first DFT-D3 (B3LYP/6-31G(d)) method and then DFT-D3/SMD method with the same basis [32]. In the case of the appearance of imaginary frequencies of normal coordinates, the optimization was repeated. The thermodynamic parameters were calculated at 298 K and 1 atm. The images were prepared using Chemcraft software [33].

## Conclusions

The detailed DFT calculations of the interaction of cucurbiturils (Q6, Q7, Q8) with Ca and Ba chlorides and iodides were performed for the first time. The thermodynamic parameters for the formation of host–guest complexes were defined. The structures of the complexes with one or two guest molecules were established. It was shown that two molecules of  $\text{CaCl}_2$  fully enclose both entries to the Q6 cavity. In the complexes of Q7 and Q8 with  $\text{CaCl}_2$ ,  $\text{CaI}_2$ ,  $\text{BaCl}_2$ , and  $\text{BaI}_2$ , the entries to the cucurbituril interior remain partially open. The formation of the bond between Q7 and  $\text{BaI}_2$  distorts a cylindrical shape of the cucurbituril. In the complex of Q8 with  $\text{BaI}_2$ , the cavitand geometry is also distorted.

The interaction of Q7 with hydrated Be and Ba cations was explored. For the model reactions, the energy parameters of the transfer of  $\text{Be}^{2+}$  and  $\text{Ba}^{2+}$  cations from an aqueous solution into the Q7 cavity containing  $n$  water molecules were calculated. The dependences of the energy of complex formation for  $\text{Q7W}_n\text{Be}^{2+}$  and  $\text{Q7W}_n\text{Ba}^{2+}$  on the number of water molecules were found to be parabolic, with the energy minima at  $n = 5$  and  $n = 6$ , respectively.

Based on the thermodynamic parameters, Q7 was shown to be able to form in an aqueous solution supramolecular complexes with mono- and diprotonated HA as well as neutral HA in the presence of  $\text{Ca}^{2+}$  ions.

## Acknowledgements

This work was performed with financial support from the Ministry of Science and Higher Education of the Russian Federation using the equipment of the Center for Molecular Composition Studies of INEOS RAS.

## Corresponding author

\* Email: sergkis@gmail.com. Tel: +7(499)135-8253

## Electronic supplementary information

Electronic supplementary information (ESI) available online: results of the computational study of the compounds under consideration; structure of complex Q7–HA– $2\text{Ca}^{2+}$ –W4. For ESI, see DOI: 10.32931/io2109a

## References

- O. A. Gerasko, V. P. Fedin, *Russ. J. Inorg. Chem.*, **2011**, *56*, 2025–2046. DOI: 10.1134/S003602361113002X
- W. M. Nau, M. Florea, K. I. Assaf, *Isr. J. Chem.*, **2011**, *51*, 559–577. DOI: 10.1002/ijch.201100044
- H. J. Buschmann, E. Cleve, L. Mutihac, E. Schollmeyer, *J. Inclusion Phenom. Macrocycl. Chem.*, **2009**, *65*, 293. DOI: 10.1007/s10847-009-9580-3
- Yu. A. Borisov, S. S. Kiselev, *Comput. Theor. Chem.*, **2021**, *1197*, 113141. DOI: 10.1016/j.comptc.2020.113141
- Y.-M. Jeon, J. Kim, D. Whang, K. Kim, *J. Am. Chem. Soc.*, **1996**, *118*, 9790–9791. DOI: 10.1021/ja962071x
- W. A. Freeman, *Acta Crystallogr., Sect. B: Struct. Sci.*, **1984**, *40*, 382–387. DOI: 10.1107/S0108768184002354
- F. Pichierri, *Dalton Trans.*, **2013**, *42*, 6083–6091. DOI: 10.1039/c2dt32180g
- V. Sinha, M. Sundararajan, *AIP Conf. Proc.*, **2014**, *1591*, 1708. DOI: 10.1063/1.4873085
- G. Zhang, A.-H. Emwas, U. F. Shahul Hameed, S. T. Arold, P. Yang, A. Chen, J.-F. Xiang, N. M. Khashab, *Chem*, **2020**, *6*, 1082–1096. DOI: 10.1016/j.chempr.2020.03.003
- H. Lambert, Y.-W. Zhang, T.-C. Lee, *J. Phys. Chem. C*, **2020**, *124*, 11469–11479. DOI: 10.1021/acs.jpcc.0c02012
- L. Mikulu, R. Michalicova, V. Iglesias, M. A. Yawer, A. E. Kaifer, P. Lubal, V. Sindelar, *Chem. Eur. J.*, **2016**, *23*, 2350–2355. DOI: 10.1002/chem.201604417
- A. D. Bani-Yaseen, *Comput. Theor. Chem.*, **2020**, *1191*, 113026. DOI: 10.1016/j.comptc.2020.113026
- N. Kircheva, S. Dobrev, L. Dasheva, I. Koleva, V. Nikolova, S. Angelova, T. Dudev, *RSC Adv.*, **2020**, *47*, 28139–28147. DOI: 10.1039/d0ra04387g
- E. Y. Chernikova, A. Y. Ruleva, V. B. Tsvetkov, Yu. V. Fedorov, V. V. Novikov, T. M. Aliyeu, A. A. Pavlov, N. E. Shepel, O. A. Fedorova, *Org. Biomol. Chem.*, **2020**, *18*, 755–766. DOI: 10.1039/C9OB02543J
- O. A. Fedorova, E. Y. Chernikova, S. V. Tkachenko, A. I. Grachev, I. A. Godovikov, Yu. V. Fedorov, *J. Inclusion Phenom. Macrocyclic Chem.*, **2019**, *94*, 201–210. DOI: 10.1007/s10847-019-00900-2
- P.-H. Shan, Z.-R. Zhang, D. Bai, B. Bian, Z. Tao, X. Xiao, *New J. Chem.*, **2019**, *43*, 407–412. DOI: 10.1039/c8nj04697b
- M. Diaz, B. del Rio, V. Ladero, B. Redruello, M. Fernández, M. Cruz Martín, M. A. Alvarez, *Int. J. Food Microbiol.*, **2015**, *215*, 117–123. DOI: 10.1016/j.ijfoodmicro.2015.08.026
- T. Baba, T. Matsui, K. Kamiya, M. Nakano, Y. Shigeta, *Int. J. Quantum Chem.*, **2014**, *114*, 1128–1134. DOI: 10.1002/qua.24631
- J. W. Steed, J. L. Atwood, *Supramolecular Chemistry*, 2nd ed., Wiley, Chichester, **2009**.
- R. G. Parr, Y. Yang, *Density-Functional Theory of Atoms and Molecules*, Oxford Univ. Press, New York, Oxford, **1989**.
- A. D. Becke, *Phys. Rev. A*, **1988**, *A38*, 3098–3100. DOI: 10.1103/PhysRevA.38.3098
- C. Lee, W. Yang, R. G. Parr, *Phys. Rev. B*, **1988**, *37*, 785–789. DOI: 10.1103/PhysRevB.37.785

23. J.-D. Chai, M. Head-Gordon, *Phys. Chem. Chem. Phys.*, **2008**, *10*, 6615–6620. DOI: 10.1039/B810189B
24. Gaussian 09, <http://www.gaussian.com>.
25. Yu. A. Borisov, S. S. Kiselev, *Dokl. Phys. Chem.*, **2015**, *463*, 168–172. DOI: 10.1134/S0012501615080023
26. Yu. A. Borisov, S. S. Kiselev, *Russ. J. Phys. Chem. A*, **2016**, *90*, 1822–1827. DOI: 10.1134/S0036024416090065
27. S. S. Kiselev, Yu. A. Borisov, *J. Struct. Chem.*, **2016**, *57*, 849–854. DOI: 10.1134/S0022476616050012
28. L. V. Snegur, Yu. A. Borisov, Yu. V. Kuzmenko, V. A. Davankov, M. M. Ilyin, M. M. Ilyin, Jr., D. E. Arhipov, A. A. Korlyukov, S. S. Kiselev, A. A. Simenel, *Molecules*, **2017**, *22*, 1410. DOI: 10.3390/molecules22091410
29. S. S. Kiselev, L. V. Snegur, A. A. Simenel, V. A. Davankov, M. M. Il'in, Yu. A. Borisov, *Russ. J. Phys. Chem. A*, **2017**, *91*, 2415–2420. DOI: 10.1134/S0036024417120123
30. J. Cioslowski, *J. Am. Chem. Soc.*, **1989**, *111*, 8333–8336. DOI: 10.1021/ja00204a001
31. V. Mukherjee, T. Yadav, *Spectrochim. Acta, Part A*, **2016**, *165*, 167–175. DOI: 10.1016/j.saa.2016.04.041
32. A. V. Marenich, C. J. Cramer, D. G. Truhlar, *J. Phys. Chem. B*, **2009**, *113*, 6378–6396. DOI: 10.1021/jp810292n
33. <http://chemcraftprog.com/>

This article is licensed under a Creative Commons Attribution-NonCommercial 4.0 International Licence.

